FEBS Letters 580 (2006) 4777–4783

NMR studies of the fifth transmembrane segment of Na^+,K^+-ATPase reveals a non-helical ion-binding region

Jarl Underhaug[a], Louise Odgaard Jakobsen[b,1], Mikael Esmann[b], Anders Malmendal[a], Niels Chr. Nielsen[a,*]

[a] *Center for Insoluble Protein Structures (inSPIN), Interdisciplinary Nanoscience Center (iNANO), Department of Chemistry, University of Aarhus, Langelandsgade 140, DK-8000 Aarhus C, Denmark*

[b] *Department of Biophysics, Institute of Physiology and Biophysics, University of Aarhus, Ole Worms Allé 1185, DK-8000 Aarhus C, Denmark*

Received 5 April 2006; revised 7 July 2006; accepted 13 July 2006

Available online 4 August 2006

Edited by Miguel De la Rosa

Abstract **The structure of a synthetic peptide corresponding to the fifth membrane-spanning segment (M5) in Na^+,K^+-ATPase in sodium dodecyl sulfate (SDS) micelles was determined using liquid-state nuclear magnetic resonance (NMR) spectroscopy. The spectra reveal that this peptide is substantially less α-helical than the corresponding M5 peptide of Ca^{2+}-ATPase. A well-defined α-helix is shown in the C-terminal half of the peptide. Apart from a short helical stretch at the N-terminus, the N-terminal half contains a non-helical region with two proline residues and sequence similarity to a non-structured transmembrane element of the Ca^{2+}-ATPase. Furthermore, this region spans the residues implicated in Na^+ and K^+ transport, where they are likely to offer the flexibility needed to coordinate Na^+ as well as K^+ during active transport.**

Keywords: Na^+,K^+-ATPase; Fifth transmembrane segment M5; Membrane protein; Transmembrane helix; Ion binding; Micelle; Nuclear magnetic resonance; Sodium dodecyl sulfate

1. Introduction

P-type ATPases are fundamental for the maintenance of electrochemical gradients of cations across the plasma membrane of most animal cells. For example, the Na^+,K^+-ATPase couples the hydrolysis of ATP with active pumping of 3 Na^+ out of the cell and 2 K^+ in the opposite direction, hereby creating a sodium gradient which is necessary in, e.g., cell homeostasis, for the uptake of nutrients, and for the establishment of a membrane potential. These aspects have rendered the so-called sodium pump a major object of research since its discovery by Skou in the fifties [1]. A large body of biophysical studies has been performed (recent reviews [2–4]), but still the detailed mechanism of the cation transport and its physiological regulation is largely unknown. One of the reasons is that apart from X-ray [5] and NMR [6] structures of the extracellular nucleotide binding (N) domain and lower resolution cryo-EM structures of the full protein [7,8], no high-resolution structure is available for the Na^+,K^+-ATPase. In lack of this, recent studies have based their discussions on homology modelling [9–12] using X-ray structures of the related sarco/endoplasmic reticulum Ca^{2+}-ATPase (SERCA) [13–16]. These studies may then be held up against what is known from biophysical and mutation studies of the Na^+,K^+-ATPase to evaluate reliability.

Relatively strong evidence exists that the overall architecture of the pumping machinery, involving the A, N, and P extramembranal domains, is very similar for all P-type ATPases, and the sequence conservation is very high in these domains. This implies that the observations for SERCA along with mutational and biophysical data most likely provide a reliable model for the function of these domains. In contrast, this clear picture does not apply to the cation binding sites in the transmembrane part of the protein. It is evident that the flexibility of the helices and steric effects play a major role for the cation selectivity and transport which probably is very specific for each P-type ATPase [4]. For example, the sizes, coordination properties, and numbers of cations involved in the pumping of the Na^+,K^+-, H^+,K^+-, and Ca^{2+}-ATPases are quite different, calling for different numbers of occlusion sites, different ion specificity, and most likely also substantially different flexibility of helices forming the frame of the occlusion sites. This implies that not only may the structural details be difficult to map from homology studies, but it should also be considered that the underlying X-ray structures provide static snapshots of the structure of selected states in the pumping cycle of SERCA. With these aspects in mind, and the knowledge that the helices M4, M5, M6, M8, and M9 contains sites involved in cation occlusion, we recently conducted an NMR analysis of the membrane spanning region of the M5 helix of SERCA (Fig. 1) in SDS micelles [17]. This study revealed a flexible region (Ile765-Asn768) interrupting the helix structure near the putative Ca^{2+} binding sites, which agrees well with biophysical data but was not seen by X-ray crystallography [13,14].

Homology studies of Na^+,K^+-ATPase relative to SERCA indicate that M5 is closely involved in both Na^+ and K^+ coordination [10,11]. On the other hand the sequence homology between M5 in the two ATPases is quite low (25% identity, 50% similarity; Fig. 2), much lower than e.g. between M5 from the Na^+,K^+- and gastric H^+,K^+-ATPases (68% identity, 86% similarity). This indicates that one might need to be cautious when using M5 in the SERCA structure as a model for M5 in the Na^+,K^+-ATPase. It is believed that for Na^+,K^+-ATPase the

*Corresponding author. Fax: +45 86 196199.
E-mail address: ncn@chem.au.dk (N.Chr. Nielsen).

[1] Present address: Cheminova A/S, DK-7673 Harboøre, Denmark.

0014-5793/$32.00
doi:10.1016/j.febslet.2006.07.063

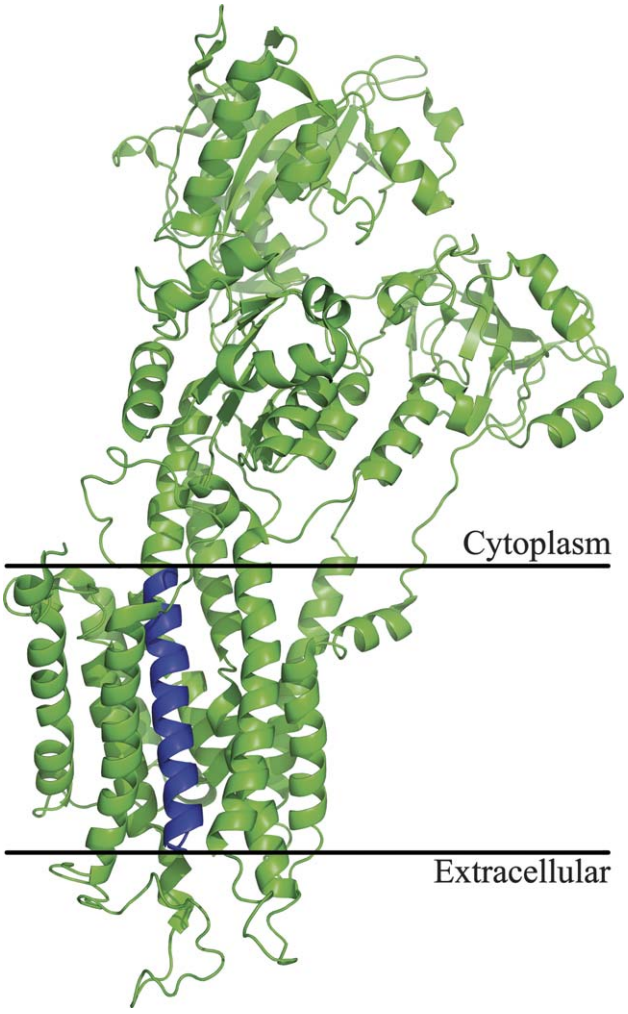

Fig. 1. The position of M5 illustrated by a ribbon representation of the X-ray structure of Ca^{2+}-free SERCA (PDB Accession Code 1IWO) [13] with the 28-residue M5 peptide emphasized in blue. Molecular graphics were prepared using PyMOL [58].

M5 residues Tyr778, Thr781, Ser782, Asn783, Pro785, Glu786, and Phe793 (Fig. 2) are involved in the monovalent cation binding, which suggests that the role of M5 here is much more involved than for the Ca^{2+}-ATPase where only two residues (Asn768 and Glu771) have been shown to play a role. The involvement of these sites and the crucial role of M5 in the cation pumping is supported by numerous studies of the Na^+,K^+-ATPase [18–21] and other ATPases [17,22–24]. To explore the homology of the M5 helices in Ca^{2+}- and Na^+,K^+-ATPases and the flexibility of these segments of importance for specific occlusion of differently sized/charged cations, this paper presents a liquid-state NMR study of the membrane spanning part of M5 of Na^+,K^+-ATPase recorded in SDS micelles under the same conditions as recently used for the same helix in Ca^{2+}-ATPase [17].

2. Materials and methods

2.1. Sample preparation

The 28-residue M5 peptide of Na^+,K^+-ATPase (Acetyl - KKSIA YTLTS NIPEI TPFLI FIIAN IPL – Amide, corresponding to Lys773–Leu800 of the fifth membrane span of Na^+,K^+-ATPase using the homo sapiens sequence; underscored residues were ^{15}N labelled) was purchased from SynPep Corporation (Dublin, CA). The peptide was synthesized using Fmoc chemistry, with the N-terminal acetylated and the C-terminus blocked by an amino group. The sequence was verified by mass spectrometry and the purity determined to be >98.2% by HPLC. The peptide was reconstituted into fully deuterated sodium dodecyl sulfate (SDS) micelles by adding M5 peptide to a solution containing 400 mM SDS-d_{25} (Cambridge Isotope Laboratories, Andover, MA), 100 mM NaCl, 20 mM sodium phosphate (pH 7.0), 1 mM NaN_3, and 10% D_2O (90% H_2O). The final peptide concentration was 2.5 mM. A second sample was prepared with 500 mM SDS-d_{25} and 5 mM peptide.

2.2. NMR spectroscopy

NMR spectra on Na^+,K^+-ATPase M5 were recorded on a Bruker Avance 400 MHz and a Varian Inova 800 MHz NMR spectrometer operating at ^1H frequencies of 400.13 and 799.81 MHz, respectively. Phase-sensitive (States-TPPI [25]) ^1H double-quantum filtered COSY (DQF-COSY) [26,27] on the 5 mM sample at 400 MHz, and TOCSY [28,29] (80 ms DIPSI-2 mixing [30]), NOESY [31,32] (200 ms mixing), and ^{15}N–^1H HSQC-NOESY [33] experiments on the 2.5 mM sample at 800 MHz were recorded at 313 K. The water signal was suppressed using weak presaturation (2 s). All spectra were recorded with a spectral width of 6361 and 11 000 Hz (400 and 800 MHz, respectively) in the ^1H, and 791 Hz (800 MHz) in the ^{15}N dimensions. Data matrices were zero-filled to double size in both dimensions. The DQF-COSY spectra were apodized using a sine-square window function shifted by $\pi/4$, while a cosine window function was applied in both dimensions of the other spectra. All spectra were processed using *NMRPipe* [34] and analysed using *SPARKY* [35].

2.3. Structure calculations

The secondary structure of the peptide was analysed qualitatively using and $^1H^\alpha$ chemical shift indexes (CSI) [36,37]. The structure calculation was performed with *ARIA 1.2* [38] in combination with *Crystallography & NMR System (CNS)* [39]. Using torsion angle dynamics and distance restraints derived from the 200 ms NOESY spectrum a final set of 100 structures were generated. The ten structures with lowest energy were analysed further.

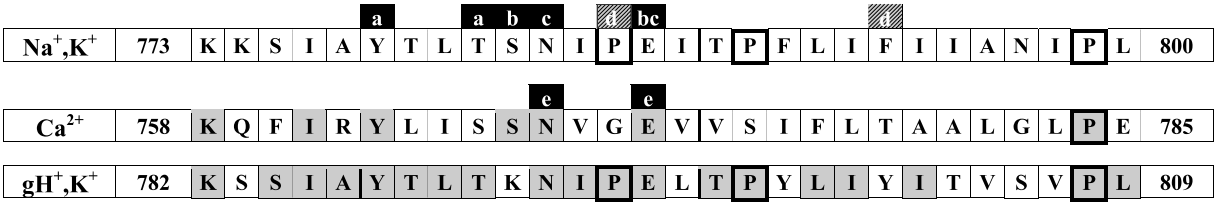

Fig. 2. Comparison of the primary sequences of the membrane spanning part of the M5 peptides in Na^+,K^+-, Ca^{2+}-, and gastric H^+,K^+-ATPase. For the two latter sequences, the shaded fields indicate residues identical with those in the Na^+,K^+-ATPase. Prolines are highlighted by solid-boxes. Putative cation binding sites are marked with dark boxes above the residue with the black fields being predicted by homology modelling [10,11] and experimental studies [18–20] (a: Na^+(III), b: K^+(I), c: K^+(II) and Na^+(I), e: Ca^{2+} binding), while mutation studies [48] includes the shaded fields as potential K^+ binding sites (d). The first and last residue positions of the M5 segments are given in the first and last columns.

3. Results

A low helical propensity of the M5 peptide of Na^+,K^+-ATPase is apparent from the amino acid sequence. Analysis using *PredictProtein* [40,41] suggests that the M5 peptide has only 50% α-helix and 21.5% β-sheet structure (Fig. 3e). Two α-helical regions are predicted, for Thr779-Thr782 and Pro785-Ile794, respectively. For comparison, the Ca^{2+}-ATPase M5 peptide was predicted to have 75% α-helix and no β-sheet structure. For the Ca^{2+}-ATPase this is in reasonable agreement with CSI values, and with the calculated NMR structure [17].

Using the ^{15}N-labeled residues in the HSQC-NOESY spectrum as a starting point, an almost complete assignment of the ^1H resonances for the Na^+,K^+-ATPase M5 peptide was achieved. All the backbone protons and about 90% of the side-chain protons were assigned. The H^α CSI [36,37] values (Fig. 3c) reveal a short α-helix between Phe790 and Ala796, but otherwise there are no clear indications of secondary structure.

Examination of the NOESY spectra for the Na^+,K^+-ATPase M5 peptide reveals that there is a limited number of medium range NOEs which can confirm the presence of α-helical structure components (Fig. 3a). The fact that only a limited number of medium range NOEs can be identified may be ascribed to signal overlap due to low chemical shift dispersion in this region. The presence of ten of the characteristic αN(i,i + 3) and αβ(i,i + 3) cross-peaks indicate that there is an α-helical region extending over the residues Pro789-Ala796, in agreement with CSI data. There is also tendency to a short helix in the N-terminus of the peptide. An excerpt from the spectral region where the αβ cross-peaks appear can be seen in Fig. 4a.

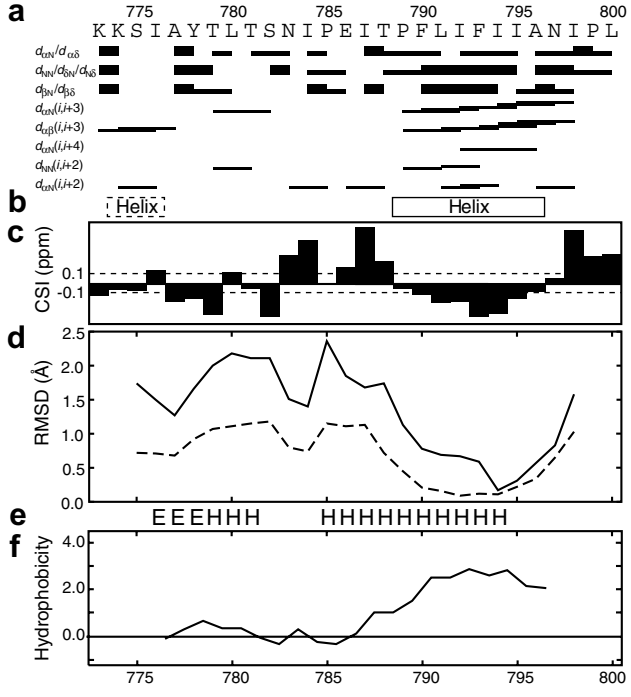

Fig. 3. Structural parameters for the Na^+,K^+-ATPase M5 peptide in SDS micelles. (a) Sequential and medium range NOEs with thicker lines indicating higher intensity. (b) The helical regions of the calculated structures as indicated by DSSP [43]. The N-terminal helix is only present in half of the calculated structures. (c) H^α chemical shift index (CSI). The low shifts of residues Phe790 to Ile795 are indicative of α-helical structure in this region. (d) RMSDs of five consecutive residues as a function of the middle residue. The solid and dashed lines represent all heavy atoms, and N, C′ and C^α atoms, respectively. (e) Helix (H) and extended (E) structure propensities obtained using the PredictProtein software [40,41]. (f) Hydrophobicity plot using a window of 8 residues [59].

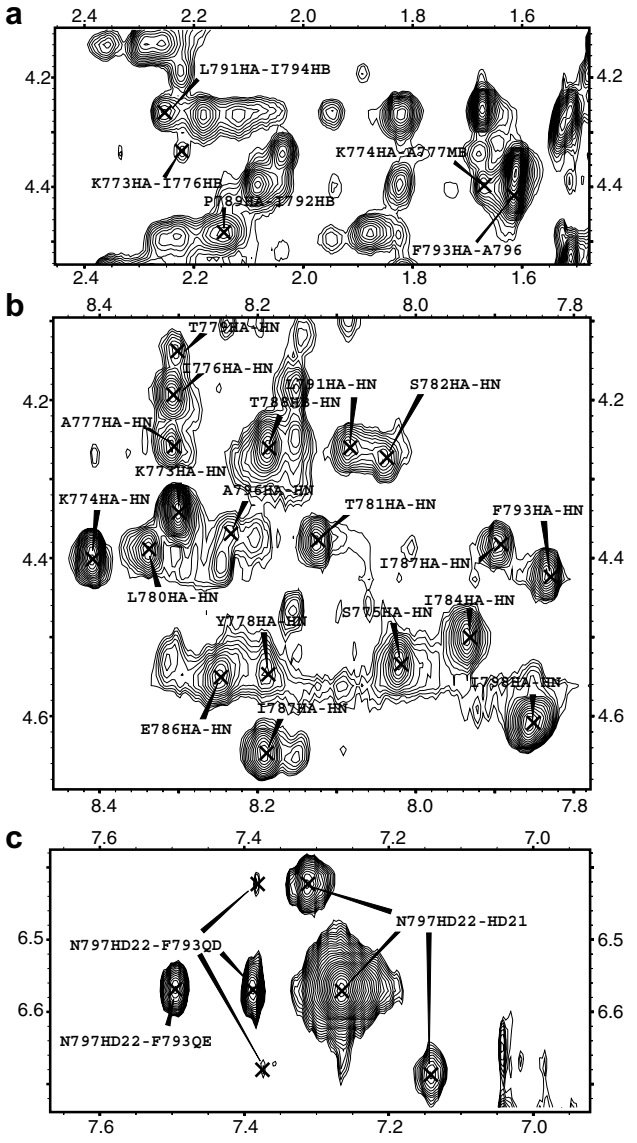

Fig. 4. Selected regions of NMR spectra for the Na^+,K^+-ATPase M5 peptide. (a) NOESY H^α–H^β-region showing five of the αβ(i,i + 3) cross-peaks characteristic for an α-helix. (b) TOCSY fingerprint region. All major H^α–H^N cross-peaks has been identified, but there are still unidentified minor peaks in this region. (c) Multiple NOESY Asn797$H^{\delta21}$–$H^{\delta22}$ cross-peaks.

A total of 473 distance restraints (232 intra-residual, 145 sequential, 88 medium range and 8 long range) were used to generate 100 structures. The ten lowest-energy structures (Fig. 5) violated on average 75 of the distance restraints with an RMS of the violations of around 0.05 Å, and an average of 3 violations greater than 0.3 Å. Analysis of the structures by PROCHECK-NMR [42] showed that the backbone torsion angles for 45.2%, 46.1%, 8.7%, and 0.0% of the residues are in 'most favoured', 'additional allowed', 'generously allowed',

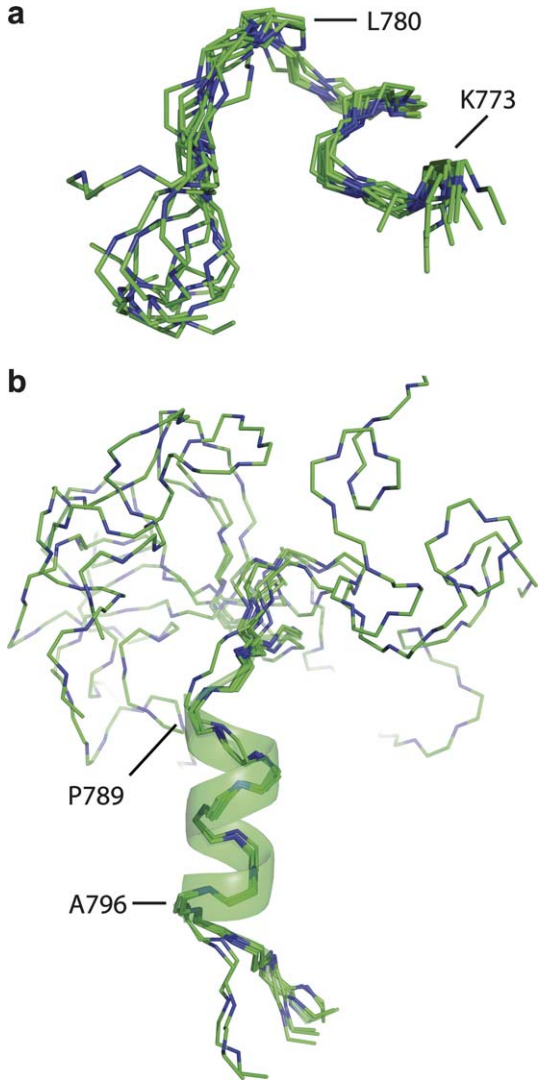

Fig. 5. Superposition of the 10 lowest-energy structures calculated for the Na^+,K^+-ATPase M5 peptide in SDS micelles. (a) Backbone atoms of the N-terminal residues Lys773 to Glu786, aligned using the backbone atoms of residues Lys773 to Leu780, showing a short helical structure. (b) All backbone atoms aligned using the backbone atoms of residues Pro789 to Ala796.

and 'disallowed regions', respectively. The structure is composed of two ordered regions connected by a more disordered region between Asn783 and Thr788. While the C-terminal region is helical, the N-terminal region does not convey to any regular type of secondary structure, except for what according to DSSP [43] is a short 3_{10} helix in the N-terminus of the peptide (Fig. 3b). The overall RMSD was 5.2 and 6.0 Å for backbone atoms and all the heavy atoms, respectively. The corresponding numbers for the N- and C-terminal regions (Lys773-Ser782 and Pro789-Ile798) were 1.0 and 2.2 Å and 0.3 and 0.7 Å, respectively. From the calculated structures, it thus appears that the N-terminal part of the M5 peptide is less ordered than the C terminal, in agreement with the presence of helical structure in this region. This is also illustrated by the backbone RMSDs of any consecutive 5 residues (Fig. 3d).

While most of the amide protons in the peptide had a line width of 28 ± 3 Hz, the N-terminal residues Lys773-Ser775 had significantly smaller line widths (15–20 Hz) indicative of a shorter correlation time. This suggests that the N-terminus is sticking out of the micelle; an observation which is compatible with the hydropathy plot in Fig. 3f, showing a quite noticeable decrease in hydrophobicity going from the C to the N terminal of the M5 peptide.

A number of extra resonances of lower intensity revealed the existence of significantly populated minor conformations, e.g. in the fingerprint region of the TOCSY spectrum (Fig. 4b) where a lot of weak H^N–H^α cross-peaks were present. Another, more striking, evidence of multiple conformers was extra Asn797$H^{\delta21}$–$H^{\delta22}$ cross-peak in the NOESY and the TOCSY spectra from two less populated conformations (Fig. 4c). The volumes of the minor cross-peaks indicate a total population of about 10% for these states.

4. Discussion

The lack of α-helicity for a large part of the Na^+,K^+-ATPase M5 peptide structure in the membrane-mimicking SDS micelle environment is interesting for several reasons. Despite the fact that the peptide is not in its native environment, and thereby lacks interactions with the surrounding transmembrane helices, there is substantial evidence that structures determined for helical fragments of proteins like bacteriorhodopsin, rhodopsin, F_1F_0-ATPase, and also the M6 segment of the Ca^{2+} ATPase display good resemblance with integral protein structures (see [17] for references). A recent NMR study of Ca^{2+} ATPase M6 segment in detergents [44] revealed that this segment was not fully helical, as later confirmed in the X-ray structure of the Ca^{2+} ATPase [13]. Furthermore, the results for the Na^+,K^+-ATPase M5 peptide are compared to the homologous Ca^{2+}-ATPase M5 peptide which under identical conditions is largely α-helical. The relatively low content of helical structure in the N-terminal part of the Na^+,K^+-ATPase M5 peptide is in striking contrast to expectations from homology modelling [9–12], which consistently refer to M5 as a regular α-helix with cations interacting with backbone or side chain donor atoms. Obviously, these deviations should be seen in the light of the low homology between the Na^+,K^+- and Ca^{2+}-ATPase M5 peptides (Fig. 2), and that the Na^+,K^+-ATPase must accommodate monovalent rather than divalent cations. It is important to note that the lack of regular secondary structure for the isolated peptide in SDS micelles does not necessarily imply that there is no secondary structure in the context of the surrounding helixes in the native protein. However, the appearance of what seems to be a more flexible or non-helical structure in the N-terminal half of the Na^+,K^+-ATPase M5 peptide in contrast to the Ca^{2+}-ATPase M5, suggests a more versatile structure that may prove important for a segment that is expected to be involved in binding to two to three Na^+ and two K^+ compared to two Ca^{2+} ions only. In this context it is also interesting to note that the flexible region of M5 has a very similar location in the membrane as the flexible region found in the M6 helix of Ca^{2+}-ATPase [44] and that the two are closely packed in the structure. Furthermore, unstructured segments are indeed found in the transmembrane regions, as exemplified by the 307-IPEGLP segment which interrupts the M4 helix in the Ca^{2+}-ATPase [10,13,14] (*vide infra*).

Although the putative Na^+ ligands in M5 of the Na^+,K^+-ATPase may not necessarily be homologous to the Ca^{2+} ligands in M5 of the Ca^{2+}-ATPase, e.g. due to different

preference for ligands of monovalent and divalent cations (e.g. [45]), homology modelling based on the Ca^{2+}-ATPase structures may be useful for determining which residues that are important in the transport process. Complementary to this, there is a significant body of mutational data. Homology modelling suggest that Asn783 and Glu786 are involved in the Na^+(I) site (using the nomenclature of Ogawa and Toyoshima [10], Fig. 2). The RMSD plots in Fig. 3d indicate substantial disorder in this region. This is in full accord with the finding of a flexible hinge in this region of the Ca^{2+}-ATPase M5 helix [17]. The second Na^+ site (II) is not expected to involve the M5 helix, while the Na^+(III) site is expected to involve Tyr778 and Thr781 [10,21] either through direct binding or control of the ion access from the cytoplasmic side. In addition, Imagawa et al. [46] have recently shown that the Thr781Ala mutations lead to a decreased Na^+ affinity. For the potassium ions, the K^+(I) site is believed to involve the residues Ser782 and Glu786 while K^+(II) involves Asn783 and Glu786 [10]. The mutation Pro785Ala leads to a reduced K^+ affinity [47], and the mutation Phe793Leu has a very high affinity for K^+ [48], suggesting that these residues are involved in K^+ binding. We note that all of these residues except Phe793 are located in the non-helical region.

An important difference to the Ca^{2+}-ATPase M5 is the two prolines at position 785 and 789 close to the centre of the transmembrane span. In contrast to helices in globular proteins, transmembrane helices often contain prolines, though they prevent formation of $(i-4,i)$ and $(i-3,i+1)$ hydrogen bonds [49]. This leads to increased flexibility, and hinges are often induced between 0 and 4 residues N-terminal of the proline and with kink angles varying with the protein context [50]. Similarly, proline insertions in isolated helical stretches often have a helix breaking effect [51]. Appearance of two prolines or a glycine and a proline such as in Pro-x-Pro and Gly-x-x-Pro motifs have been shown to be associated with hinge-bending motions in transmembrane helices [52]. It has been speculated for [2,53] and against [10] that the M5 helix of the Na^+,K^+-ATPase may be interrupted because of the similarity of the 784-IPEITP segment with the 307-IPEGLP segment in the Ca^{2+}-ATPase which interrupts the M4 helix in the X-ray structures [10,13,14]. It is noteworthy that the positions of these regions in the membrane are very similar.

Overall, the putative Na^+ and K^+-binding sites are believed to involve 6 out of 9 residues in the region Tyr778-Glu786 with a sequence-controlled specificity for cation type to accomplish transport. Looking at the NOE and CSI data in Fig. 3a, it is clear that this region is very unstructured in the SDS micelle associated M5 peptide and thereby has the necessary versatility to accommodate such transfers.

A rather dynamic nature of this segment and surprisingly low stabilizing effect from the surrounding structure is indicated by the fact that the M5–M6 hairpin of the Na^+,K^+-ATPase has been shown to release irreversibly from the membrane upon heating in the absence of cations [18]. Furthermore, a recent real-time voltage clamp fluorimetry study of the Na^+,K^+-ATPase, with a fluorescence probe attached to Asn797, revealed considerable conformational dynamics of the M5 helix during Na^+/Na^+ exchange in the E_1P–E_2P reaction cycle [19]. Last but not least: Pro785Leu and Pro789Leu mutations had drastic effects on the behaviour of the Na^+,K^+-ATPase [47,54]. The mutations actually had a positive effect on the insertion of a segment ranging from the N-terminus to the end of M5 (until Gly813) into membranes in *Xenopus* oocytes [54]. They thus behave as predicted, disturbing the helicity and thereby the membrane interactions, allowing for a number of less membrane-affine conformations of M5. On the other hand, Pro785Leu abolished transport function and Pro789Leu reduced it by 50% [54]. The prolines and the flexibility they induce are thus essential for the function.

Another characteristic of prolines is their ability to isomerise between *cis* and *trans* conformation [55]. *Cis–trans* isomerism at the prolines is likely to be a major source of the multiple conformations of the M5 peptide apparent from the NMR spectra (Figs. 4b and c). In the case of Asn797 this is likely to be dominated by the adjacent Pro799, but similar effects are seen for residues around Pro785 and Pro789. A recent study of the pore of a neurotransmitter-gated ion channel could link transmitter binding to proline *cis–trans* isomerization [56], and it was shown that a peptide construct containing this proline in SDS micelles was in equilibrium between these two states. It is not unlikely that the alternative conformations seen in this peptide are relevant for the function of the Na^+,K^+-ATPase. Our finding that the N-terminus of M5 sticks out of the detergent micelle suggests that the remainder of the peptide is embedded in the hydrophobic interior. Burial of the C-terminal end in the micelle agrees with the disposition of native M5, where labelling with sulfhydryl reagents from the aqueous phase is possible for residues Gly803-Val805 in mutated M5 [57], but not for Pro801 and Leu802.

In summary, we conclude that part of the M5 segment from the Na^+,K^+-ATPase has significantly lower helical propensity than the corresponding peptide in the Ca^{2+}-ATPase. This can be concluded from liquid-state NMR studies of the two M5 peptides in SDS micelles, of which only the Ca^{2+}-ATPase data can be compared to existing X-ray structures. For the Ca^{2+}-ATPase M5 peptide an earlier study revealed high similarity to the crystal structure, with the notable exception of a flexible hinge region in proximity of the putative Ca^{2+}(I) binding site – a flexibility that was supported by biophysical investigations [17]. For both peptides the NMR studies address structural properties of isolated peptides in membrane-mimicking environments rather than in the compact protein environment with stabilizing helix–helix interactions. Even with these precautions, it is remarkable that the M5 peptide from the Na^+,K^+-ATPase display a much lower degree of helical structure than the corresponding Ca^{2+}-ATPase peptide, and that the flexible region overlaps with most residues implicated to be involved in ion transport. This indicates that the peptide can rearrange without excessive energy cost during occlusion and transmembrane transport of the cations. This flexibility might be fundamental for the ability of the Na^+,K^+-ATPase to transport Na^+ and K^+ through the membrane with high cation-specificity.

5. Supporting material

^1H and ^{15}N chemical shifts for the Na^+,K^+-ATPase M5 peptide in SDS micelles have been deposited in the BioMagResBank (BMRB Accession Code 7049).

Acknowledgements: We acknowledge the Danish Center for NMR of Biological Macromolecules at the Carlsberg Laboratory for the use of the Varian Inova 800 MHz spectrometer. This research was funded

by Danish National Research Foundation, The Danish Biotechnological Instrument Centre (DABIC), The Danish Natural Science Council, Aarhus University Research Foundation, and Carlsbergfondet.

References

[1] Skou, J.C. (1957) The influence of some cations on an adenosine triphosphatase from peripheral nerves. Biochem. Biophys. Acta 23, 394–401.

[2] Møller, J.V., Juul, B. and le Maire, M. (1996) Structural organization, ion transport, and energy transduction of P-type ATPases. Biochim. Biophys. Acta 1286, 1–51.

[3] Jørgensen, P.L., Håkansson, K.O. and Karlish, S.J.D. (2003) Structure and mechanism of Na,K-ATPase: functional sites and their interactions. Annu. Rev. Physiol. 65, 817–849.

[4] Horisberger, J.-D. (2004) Recent insights into the structure and mechanism of the sodium pump. Physiology 19, 377–387.

[5] Håkansson, K.O. (2003) The crystallographic structure of Na,K-ATPase N-domain at 2.6 Å resolution. J. Mol. Biol. 332, 1175–1182.

[6] Hilge, M., Siegal, G., Vuister, G.W., Güntert, P., Gloor, S.M. and Abrahams, J.P. (2003) ATP-induced conformational changes of the nucleotide-binding domain of Na,K-ATPase. Nat. Struct. Biol. 10, 468–474.

[7] Hebert, H., Purhonen, P., Vorum, H., Thomsen, K. and Maunsbach, A.B. (2001) Three-dimensional structure of renal Na,K-ATPase from cryo-electron microscopy of two-dimensional crystals. J. Mol. Biol. 314, 479–494.

[8] Rice, W.J., Young, H.S., Martin, D.W., Sachs, J.R. and Stokes, D.L. (2001) Structure of Na^+,K^+-ATPase at 11-Å resolution: comparison with Ca^{2+}-ATPase in E1 and E2 states. Biophys. J. 80, 2187–2197.

[9] Sweadner, K. and Donnet, C. (2001) Structural similarities of Na,K-ATPase and SERCA, the Ca^{2+}-ATPase of the sarcoplasmic reticulum. Biochem. J. 356, 685–704.

[10] Ogawa, H. and Toyoshima, C. (2002) Homology modeling of the cation binding sites of Na^+K^+-ATPase. Proc. Natl. Acad. Sci. USA 99, 15977–15982.

[11] Rakowski, R.F. and Sagar, S. (2003) Found: Na(+) and K(+) binding sites of the sodium pump. News Physiol. Sci. 18, 164–168.

[12] Håkansson, K.O. and Jørgensen, P.L. (2003) Homology modeling of Na,K-ATPase: a putative third sodium binding site suggests a relay mechanism compatible with the electrogenic profile of Na^+ translocation. Ann. NY Acad. Sci. 986, 163–167.

[13] Toyoshima, C., Nakasako, M., Nomura, H. and Ogawa, H. (2000) Crystal structure of the calcium pump of sarcoplasmic reticulum at 2.6 Å resolution. Nature 405, 647–655.

[14] Toyoshima, C. and Nomura, H. (2002) Structural changes in the calcium pump accompanying the dissociation of calcium. Nature 418, 605–611.

[15] Sørensen, T.L.M., Møller, J.V. and Nissen, P. (2004) Phosphoryl transfer and calcium ion occlusion in the calcium pump. Science 304, 1672–1675.

[16] Toyoshima, C. and Mizutani, T. (2004) Crystal structure of the calcium pump with a bound ATP analogue. Nature 430, 529–535.

[17] Nielsen, G., Malmendal, A., Meissner, A., Møller, J.V. and Nielsen, N.C. (2003) NMR studies of the fifth transmembrane segment of sarcoplasmic reticulum Ca^{2+}-ATPase reveals a hinge close to the Ca^{2+}-ligating residues. FEBS Lett. 544, 50–56.

[18] Lutsenko, S., Anderko, R. and Kaplan, J.H. (1995) Membrane disposition of the M5–M6 hairpin of Na^+,K(+)-ATPase alpha subunit is ligand dependent. Proc. Natl. Acad. Sci. USA 92, 7936–7940.

[19] Geibel, S., Kaplan, J.H., Bamberg, E. and Friedrich, T. (2003) Conformational dynamics of the Na^+/K^+-ATPase probed by voltage clamp fluorometry. Proc. Natl. Acad. Sci. USA 100, 964–969.

[20] Burnay, M., Crambert, G., Kharoubi-Hess, S., Geering, K. and Horisberger, J.-D. (2003) Electrogenicity of Na,K- and H,K-ATPase activity and presence of a positively charged amino acid in the fifth transmembrane segment. J. Biol. Chem. 278, 19237–19244.

[21] Li, C., Capendeguy, O., Geering, K. and Horisberger, J.-D. (2005) A third Na^+-binding site in the sodium pump. Proc. Natl. Acad. Sci. USA 102, 12706–12711.

[22] Dutra, M.B., Ambesi, A. and Slayman, C.W. (1998) Structure–function relationships in membrane segment 5 of the yeast Pma1 H^+-ATPase. J. Biol. Chem. 273, 17411–17417.

[23] Koenderink, J.B., Swarts, G.P., Willems, P.H.G.M., Krieger, E. and De Pont, J.J.H.H.M. (2004) A conformation-specific interhelical salt bridge in the K^+ binding site of gastric H,K-ATPase. J. Biol. Chem. 279, 16417–16424.

[24] Swarts, H.G.P., Koenderink, J.B., Willems, P.H.G.M., Krieger, E. and De Pont, J.J.H.H.M. (2005) Asn792 participates in the hydrogen bond network around the K^+-binding pocket of gastric H,K-ATPase. J. Biol. Chem. 280, 11488–11494.

[25] Marion, D., Ikura, M., Tschudin, R. and Bax, A. (1989) Rapid recording of 2D NMR spectra without phase cycling. Application to the study of hydrogen exchange in proteins. J. Magn. Reson. 85, 393–399.

[26] Rance, M., Sørensen, O.W., Bodenhausen, G., Wagner, G., Ernst, R.R. and Wüthrich, K. (1983) Improved spectral resolution in cosy ^1H NMR spectra of proteins via double quantum filtering. Biochem. Biophys. Res. Commun. 117, 479–485.

[27] Derome, A. and Williamson, M. (1990) Rapid-pulsing artifacts in double-quantum-filtered COSY. J. Magn. Reson. 88, 177–185.

[28] Braunschweiler, L. and Ernst, R.R. (1983) Coherence transfer by isotropic mixing: application to proton correlation spectroscopy. J. Magn. Reson. 53, 521–528.

[29] Bax, A. and Davis, D.G. (1985) MLEV-17 based two-dimensional homonuclear magnetization transfer spectroscopy. J. Magn. Reson. 65, 355–360.

[30] Jeener, J., Meier, B.H., Bachmann, P. and Ernst, R.R. (1979) Investigation of exchange processes by two-dimensional NMR spectroscopy. J. Chem. Phys. 71, 4546–4553.

[31] Macura, S., Huang, Y., Suter, D. and Ernst, R.R. (1981) Two-dimensional chemical exchange and cross-relaxation spectroscopy of coupled nuclear spins. J. Magn. Reson. 43, 259–281.

[32] Shaka, A.J., Lee, C.J. and Pines, A. (1988) Iterative schemes for bilinear operators: application to spin decoupling. J. Magn. Reson. 77, 274–293.

[33] Zhang, O., Kay, L.E., Oliver, J.P. and Forman-Kay, J.D. (1994) Backbone ^1H and ^{15}N resonance assignments of the N-terminal SH3 domain of drk in folded and unfolded states using enhanced-sensitivity pulsed field gradient NMR techniques. J. Biomol. NMR 4, 845–858.

[34] Delaglio, F., Grzesiek, S., Vuister, G.W., Zhu, G., Pfeifer, J. and Bax, A. (1995) NMRPipe: a multidimensional spectral processing system based on UNIX pipes. J. Biomol. NMR 6, 277–293.

[35] Goddard, T.D. and Kneller, D.G. (2002) SPARKY-3, University of California, San Francisco.

[36] Wishart, D.S., Richards, F.M. and Sykes, B.D. (1992) The chemical shift index: a fast and simple method for the assignment of protein secondary structure through NMR spectroscopy. Biochemistry 31, 1647–1651.

[37] Wishart, D.S. and Sykes, B.D. (1994) Chemical shifts as a tool for structure determination. Meth. Enzymol. 239, 363–392.

[38] Linge, J.P., O'Donoghue, S.I. and Nilges, M. (2001) Automated assignment of ambiguous nuclear overhauser effects with ARIA. Meth. Enzymol. 339, 71–90.

[39] Brünger, A.T., Adams, P.D., Clore, M., deLano, W.L., Gros, P., Gross-Kunstleve, R.W., Jiang, J.-S., Kuszewski, J., Nilges, M., Pannu, N.S., Read, R.J., Rice, L.M., Simonson, T. and Warren, G.L. (1998) Crystallography & NMR system: a new software suite for macromolecular structure determination. Acta Crystallogr. D54, 905–921.

[40] Rost, B. and Sander, C. (1993) Prediction of protein secondary structure at better than 70-percent accuracy. J. Mol. Biol. 232, 584–599.

[41] Rost, B. (1996) PHD: predicting 1D protein structure by profile based neural networks. Meth. Enzymol. 266, 525–539.

[42] Laskowski, R.A., Rullmann, J.A., MacArthur, M.W., Kaptein, R. and Thornton, J.M. (1996) AQUA and PROCHECK-NMR: programs for checking the quality of protein structures solved by NMR. J. Biomol. NMR 8, 477–486.

[43] Kabsch, W. and Sander, C. (1983) Dictionary of protein secondary structure – pattern-recognition of hydrogen-bonded and geometrical features. Biopolymers 22, 2577–2637.
[44] Soulie, S., Neumann, J.M., Berthomieu, C., Moller, J.V., le Maire, M. and Forge, V. (1999) NMR conformational study of the sixth transmembrane segment of sarcoplasmic reticulum Ca^{2+}-ATPase. Biochemistry 38, 5813–5821.
[45] Gouaux, E. and MacKinnon, R. (2005) Principles of selective ion transport in channels and pumps. Science 310, 1461–1465.
[46] Imagawa, T., Yamamoto, T., Kaya, S., Sakaguchi, K. and Taniguchi, K. (2005) Thr-774 (transmembrane segment M5), Val-920 (M8), and Glu-954 (M9) are involved in Na^+ transport, and Gln-923 (m8) is essential for Na,K-ATPase activity. J. Biol. Chem. 280, 18736–18744.
[47] Vilsen, B. (1997) Leucine 332 at the boundary between the fourth transmembrane segment and the cytoplasmic domain of Na^+,K^+-ATPase plays a pivotal role in the ion translocating conformational changes. Biochemistry 36, 13312–13324.
[48] Vilsen, B. (1999) Mutant Phe788 → Leu of the Na^+,K^+-ATPase is inhibited by micromolar concentrations of potassium and exhibits high Na^+-ATPase activity at low sodium concentrations. Biochemistry 38, 11389–11400.
[49] von Heijne, G. (1991) Proline kinks in transmembrane alpha-helices. J. Mol. Biol. 218, 499–503.
[50] Cordes, F.S., Bright, J.N. and Sansom, M.S.P. (2002) Proline-induced distortions of transmembrane helices. J. Mol. Biol. 323, 951–960.
[51] Nilsson, I. and von Heijne, G. (1998) Breaking the camelís back: proline-induced turns in a model transmembrane helix. J. Mol. Biol. 284, 1185–1189.
[52] Tieleman, D.P., Shrivastava, I.H., Ulmschneider, M.R. and Sansom, M.S.P. (2001) Proline-induced hinges in transmembrane helices: possible roles in ion channel gating. Proteins: Struct. Funct. Genet. 44, 63–72.
[53] Pedersen, P.A., Nielsen, J.M., Rasmussen, J.H. and Jørgensen, P.L. (1998) Contribution to Tl+, K+, and Na+ binding of Asn(776), Ser(775), Thr(774), Thr(772), and Tyr(771)in cytoplasmic part of fifth transmembrane segment in alpha-subunit of renal Na,K-ATPase. Biochemistry 37, 17818–17827.
[54] Béguin, P., Hasler, U., Beggah, A., Horisberger, J.D. and Geering, K. (1998) Membrane integration of Na,K-ATPase alpha-subunits and beta-subunit assembly. J. Biol. Chem. 273, 24921–24931.
[55] Schmid, F.X. (1993) Prolyl isomerase – enzymatic catalysis of slow protein-folding reactions. Annu. Rev. Biophys. Biomol. Struct. 22, 123–143.
[56] Lummis, S.C.R., Beene, D.L., Lee, L.W., Lester, H.A., Broadhurst, R.W. and Dougherty, D.A. (2005) *Cis–trans* isomerization at a proline opens the pore of a neurotransmitter-gated ion channel. Nature 438, 248–252.
[57] Capendeguy, O. and Horisberger, J.-D. (2005) The role of the third extracellular loop of the Na+,K+-ATPase alpha subunit in a luminal gating mechanism. J. Physiol. 565, 207–218.
[58] DeLano, W.L. (2002) The PyMOL Molecular Graphics System on World Wide Web <http://www.pymol.org>.
[59] Kyte, J. and Doolittle, R. (1982) A simple method for displaying the hydropathic character of a protein. J. Mol. Biol. 157, 105–132.